Scientific Research Publishing

Open Journal of Geology, 2025, 15(9), 603-626
https://www.scirp.org/journal/ojg
ISSN Online: 2161-7589
ISSN Print: 2161-7570

Geological Characterisation and Depositional Settings of Hydrocarbon Reservoirs in the Doba Basin in Chad: Implications for Exploration and Production

Diab Ahmad Diab[1], Sanda Oumarou[2], Jean Marcel[2], Kana Janvier Domra[3*], Aretouyap Zakari[4], Franck Eitel Kemgang Ghomsi[2], Philippe Njandjock Nouck[5]

[1]Department of Physics, Teachers Training Higher School of N'Djamena, N'Djamena, Chad
[2]National Institute of Cartography, Yaoundé, Cameroon
[3]National Advance School of Mines and Petroleum Industries, University of Maroua, Kaele, Cameroon
[4]Department of Architecture and Engineering Art, Institute of Fine Arts, University of Dschang, Foumban, Cameroon
[5]Department of Physics, Faculty of Science, University of Yaoundé 1, Yaoundé, Cameroon
Email: *janvierdomra@gmail.com

How to cite this paper: Diab, D.A., Oumarou, S., Marcel, J., Domra, K.J., Zakari, A., Ghomsi, F.E.K. and Nouck, P.N. (2025) Geological Characterisation and Depositional Settings of Hydrocarbon Reservoirs in the Doba Basin in Chad: Implications for Exploration and Production. *Open Journal of Geology*, **15**, 603-626.
https://doi.org/10.4236/ojg.2025.159030

Received: May 22, 2025
Accepted: September 27, 2025
Published: September 30, 2025

Abstract

This study investigates the lithostratigraphic architecture and depositional environment of petroleum reservoirs in the Doba oil field, located in the Lake Chad Basin. Scientific research that exhibits the important geological and geophysical settings of this basin is lacking. The sedimentary fill of the Doba Basin spans from the Early Cretaceous to the Late Cretaceous, with some sequences extending into the Cenozoic. Hydrocarbon production in Doba Basin, particularly the northern boundary, for instance, has not yet succeeded due to the unawareness of its depositional environment. Understanding these geological characteristics is crucial for optimising the exploration and exploitation of petroleum resources. The research involves analysing geological, well log, core sample and petrophysical data from the oil wells to identify and correlate lithostratigraphic units across the oil field. The results show that the architecture, chronostratigraphic interval, lithostratigraphic units, and depositional environment are limited to the clay, sand, anhydrite, coal, sandstone, and limestone deposits from the base of the Cretaceous. These deposits exhibit spatio-temporal dispersion across the study area, influenced by local and/or regional tectonic controls. The identified reservoirs exhibit excellent porosity characteristics, ranging from 25% - 29.5%, and permeability generally is greater than 600 millidarcies (md). The results of this study will serve for the future prospector on the neighboring oil and gas fields of our study area. Significant advances have been

made to ensure future exploration success.

Keywords

Chad, Depositional Environment, Lithostratigraphic Architecture, Well Log, Doba Basin, Cretaceous

1. Introduction

The Doba Oil Field, located in the Lake Chad Basin, is a significant area of interest for petroleum exploration and production. This region is part of the Early and Late Cretaceous rift system that extends across much of West Central Africa [1]. The Doba Basin, along with the neighboring Dosséo Basin, forms one of the primary branches of this rift system, separated by the Borogop fault zone, a Tertiary inversion structure [1].

The Doba Oil Field development project encompasses three major oil fields: Komé, Bolobo, and Miandoum [2]. These fields are characterised by large anticlinal structures and are situated in the southern part of the Doba Basin [1] [3] [4]. The thick, regionally extensive Miandoum clays overlying the sandstone group serve as the cap rock, with the production area covering approximately 40 km by 22 km. The productive intervals in this field are primarily of Early and Late Cretaceous age, with the Upper Cretaceous reservoirs, located at depths of 1000 to 1800 meters, containing about 97% of the project's reserves [5].

This basin thus presents significant scientific and economic interest. Consequently, the Doba Basin has been the subject of geological and geophysical studies, both in outcrop and through drilling [4] [5]. These studies have provided knowledge of the basin since the Cretaceous, revealing several productive and shallow reservoirs, often located at depths of less than 2500 meters. Seismic data analysis shows a succession of major sedimentary systems and depositional environments, including the top Tarbert, Ness, and Etive formations, linking coastal and intertidal environments [4] [6]. Research on the Doba Basin has made significant progress, but there are still some gaps that need to be addressed. Scientific research that exhibits the important geological and geophysical settings of this basin is still lacking. Hydrocarbon production in Doba Basin, particularly the northern boundary, for instance, has not yet succeeded due to the unawareness of its depositional environment. While there have been studies on the hydrocarbon accumulation patterns in the Doba Basin, there is still a need for more detailed research on the specific factors controlling these patterns, such as depositional settings and reservoir-seal combinations [1].

The lacustrine environment of the Doba Basin presents unique challenges for reservoir characterization. More research is needed to understand the sedimentological complexity and the impact of radioactive sand on hydrocarbon production. Although there have been studies on the tectonic evolution of the Doba Basin, fur-

ther research is needed to fully understand the structural history and its impact on hydrocarbon distribution [5].

According to the Société des Hydrocarbures du Tchad (SHT) report, Chadian hydrocarbon production went down in 2020 and 2021. This drop-in production is mainly due to the depletion of fields. To remedy this deficit, the Chadian State has promoted several blocks in the Doba basin. Prospecting for these blocks begins with a better understanding of geological and petrophysical knowledge of neighboring or operating fields in the basin. In this context, a study on the characterization of reservoirs in the Doba basin is therefore beneficial. The exploration of new hydrocarbon reserves is known to be expensive, so it is necessary to use low-cost methods to locate and quantify these reservoirs.

This study aims to analyse the lithostratigraphic architecture and depositional environment of the petroleum reservoirs in the Doba basin. The research involves a new integrated comprehensive analysis of geological, well log, core sample, and petrophysical data from the oil wells to identify and correlate lithostratigraphic units across the oil field. Additionally, cross plots were established to better understand the lithostratigraphy and depositional environments between different wells. This combined method can be serving to broader basin with the same geological context.

2. Research Site

The Doba Basin is located in southern Chad (**Figure 1**), within the Central African Rift system. This sedimentary basin is part of the larger Lake Chad Basin and is situated in the southern part of the country. The basin is characterised by its significant petroleum resources and complex geological history (**Figure 2**), which includes up to 10 kilometers of non-marine sediments from the Early Cretaceous to the present [7].

The Doba Basin is bordered by the Borogop fault zone to the north, which separates it from the neighboring Doseo Basin. The basin's geographic coordinates roughly place it between latitudes 8˚N and 10˚N and longitudes 16˚E and 18˚E (**Figure 1**).

This region is of great economic importance due to its oil fields, including the Komé, Bolobo, and Miandoum fields, which are key contributors to Chad's petroleum production.

The basin's basement is composed of Precambrian metamorphic rocks [9] (**Figure 3**, **Figure 4**). Lower Cretaceous Formations include the Mangara, Kedeni, Doba, and Lower Kome formations, which are relatively thin and primarily consist of lacustrine sediments. These formations contain interbedded sandstones and sedimentary rocks originally composed of clay or mud, serving as major reservoir strata.

The Doba Basin and the neighboring Doseo Basin were formed as part of the Central African Rift system, which underwent multiple phases of extension and inversion [10]. The basins were initially identified using gravity data, and subsequent

exploration has significantly increased understanding of their evolution. The Borogop fault zone, a Tertiary inversion structure, separates the Doba and Doseo basins [10] [11] (**Figure 5**).

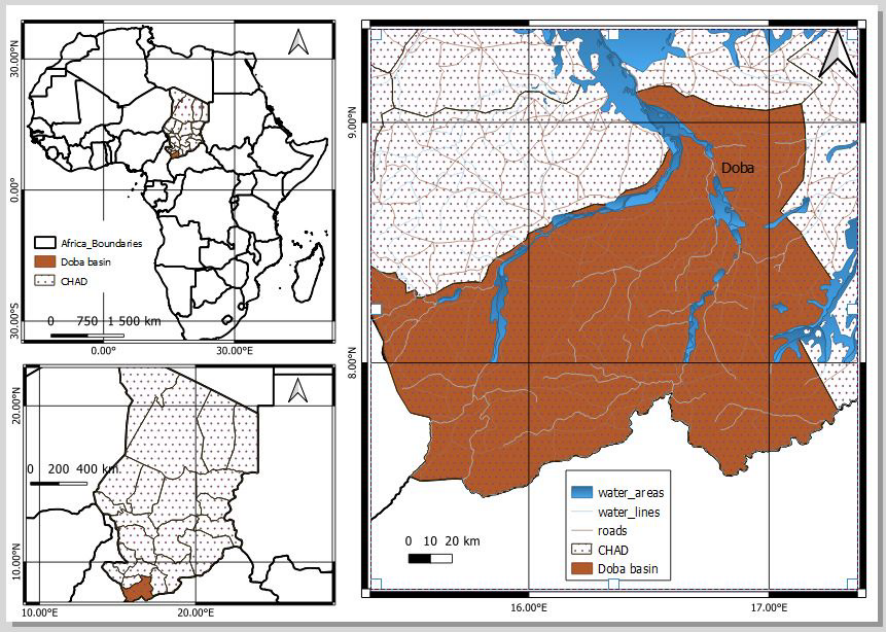

Figure 1. Study area showing Doba Bassin. Source: [4].

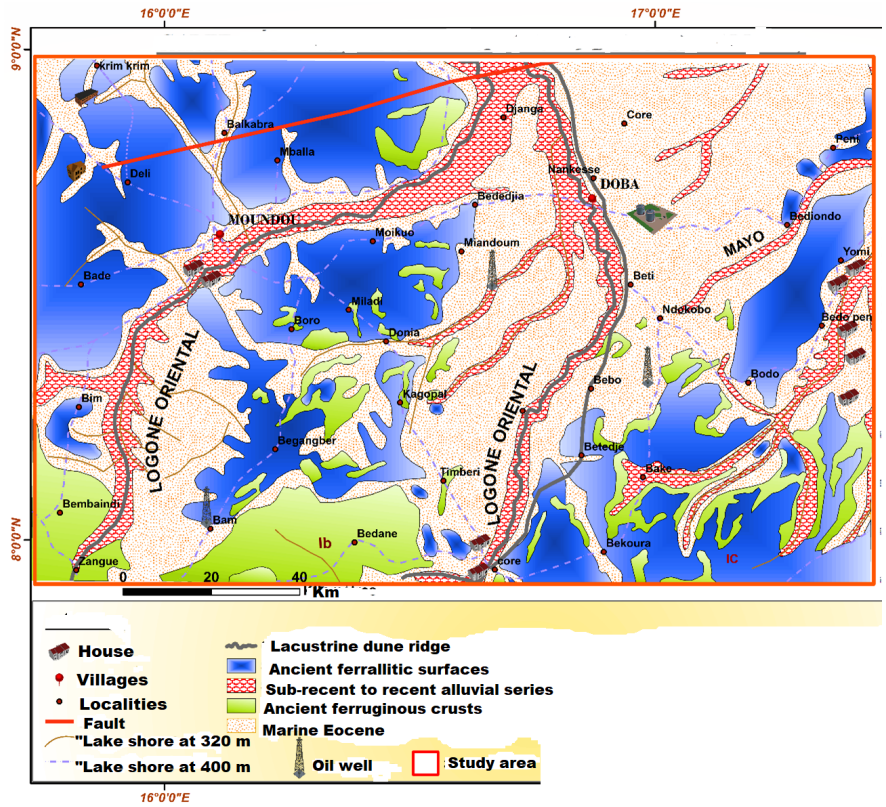

Figure 2. Geological map of the study area [7] [8]. Source: [4].

ETAGE	AGES	LITHO	DESCRIPTION
QUAT.	Quaternary		Sand
TERT.	Mio-Pliocene		white sand, limestone
CRETACE	Carbonate Senonian		limestone, dolomy, clay, anhydrite
	Anhydritic Senonian		Salt, anhydrite
	Saliferous Senonian		Salt, clay
	Turonian		Limestone, clay, dolomy
	Cenomanian		Clay, limestone, dolomy
	Albian		Sanstone, clay
	Aptian		Dolomy, limestone
	Barremian		sandstone, clay
	Neocomian		Clay, sandstone, limestone

Figure 3. Lithostratigraphy of Doba Basin [9]. Source: [4].

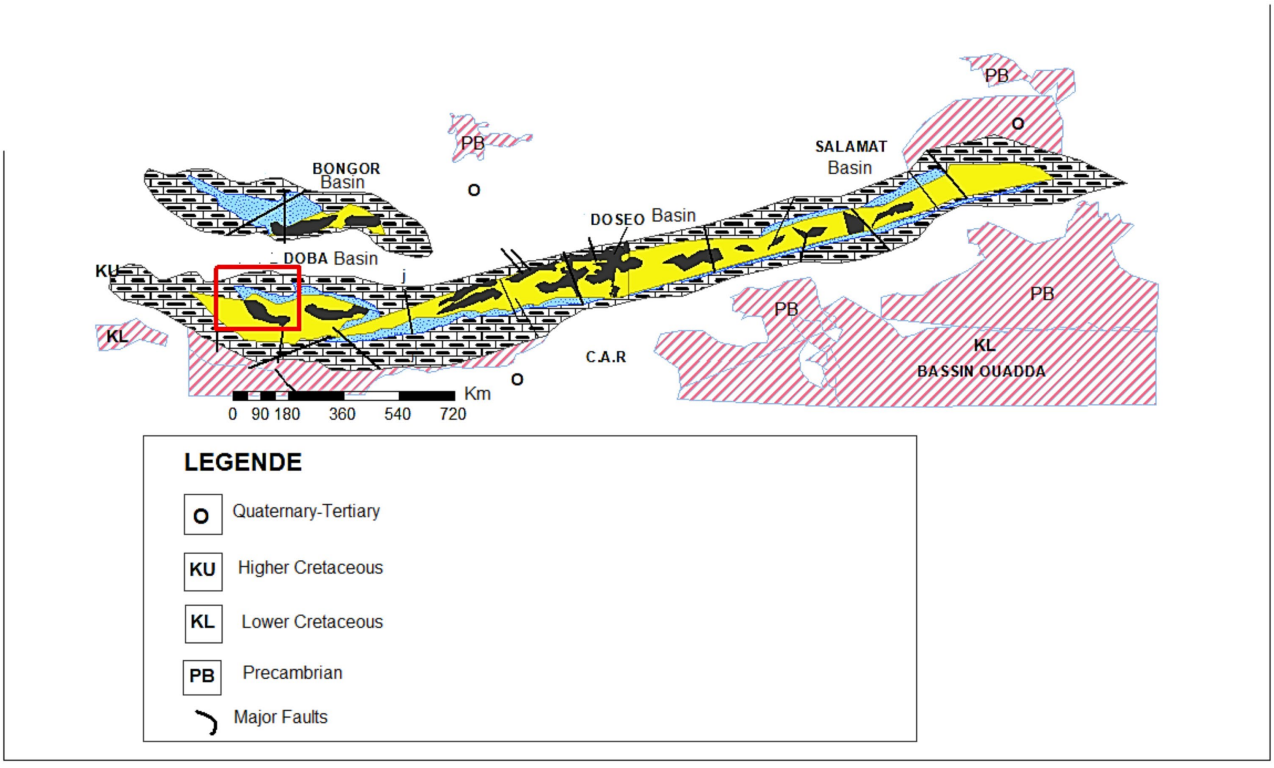

Figure 4. Geological map showing Chad Basin [9]. Source: [4].

The sequence of the Doba Basin from the Brent Group consists of three formations (**Figure 6**). The Tarbert, Ness, and Etive formations are used by most authors [12].

The Tarbert Formation represents shallow marine sandstone. Tarbert consists of facies of fine to medium-grained sandstone with thin facies of siltstones and shales.

The Ness Formation represents both a regressive part (northward shift of the Doba Basin) and a transgressive part. The Ness Formation represents a carbona-

ceous and coal-bearing sandstone. The lithology of the Ness Formation varies since the formation includes several facies, which is also the reason why the Ness Formation is the most variable unit of the Brent Group.

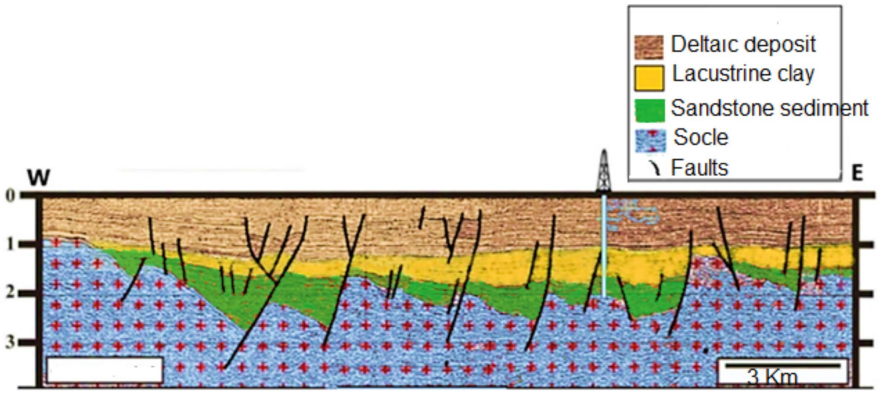

Figure 5. Geological cross-section of Doba Bassin showing faults [10] [11]. Source: [4].

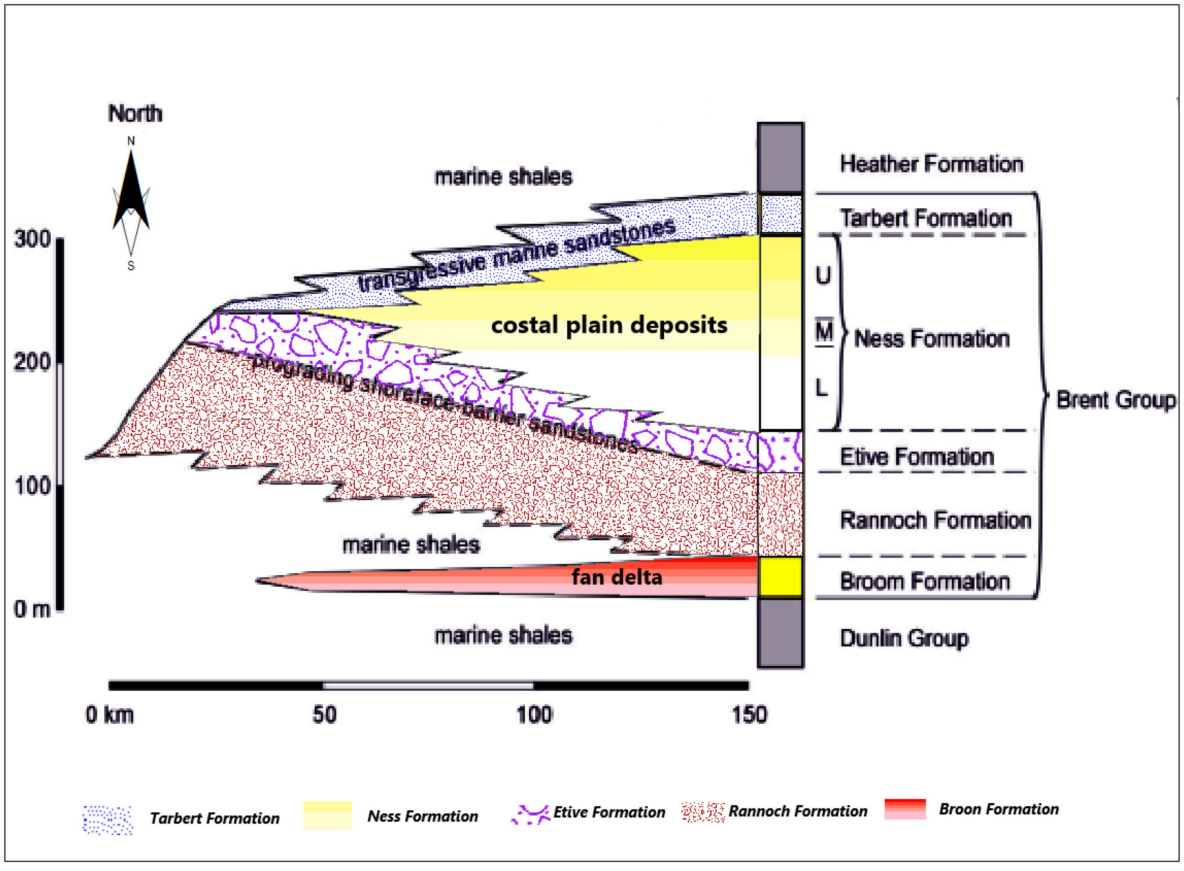

Figure 6. Depositional environment evolution (Brent Group) [12]. Source: [4].

The Etive Formation generally consists of well-sorted, medium-grained, and rather massive sands considered to have been deposited in the environments of the upper shoreface and beach of a barrier complex, with tidal channels crossing the

barrier sediments [12].

The Doba development project includes three major oil fields: Komé, Bolobo, and Miandoum. These fields are characterized by large anticlinal structures and are situated in the southern part of the Doba Basin. The thick, regionally extensive Miandoum clays overlying the sandstone group serve as the cap rock, with the production area covering approximately 40 km by 22 km [13]. The hydrocarbon accumulation in these reservoirs is influenced by the depositional settings and the combination of reservoir-seal pairs, with faults playing a crucial role in hydrocarbon trapping and lateral sealing [14].

Maintaining the Integrity of the Specifications

The template is used to format your paper and style the text. All margins, column widths, line spaces, and text fonts are prescribed; please do not alter them. You may note peculiarities. For example, the head margin in this template measures proportionately more than is customary. This measurement and others are deliberate, using specifications that anticipate your paper as one part of the entire journal, and not as an independent document. Please do not revise any of the current designations.

3. Materials and Methods

3.1. Data

The data used in this study focuses on the well log data from six wells (34_10-A-13, 34_10-A-15, 34_10-A-18, A10, B9, and C1) located in the oil fields of the Doba Basin in southern Chad. The data is provided in the LAS format log file. The acquired data includes: Caliper: Measures the borehole diameter, highlighting caved zones; Gamma Ray (GR): Measures the natural radioactivity of the formation in API units, with a scale from 0 to 150 API, indicating naturally radioactive materials; Resistivity (ILD): Measures the electrical resistivity of the formation in Ohm.m, providing information on fluid content within the formations; Density (RHOB): Measures the density within the formations; Neutron Porosity (NPHI): Measures the porosity of the formation; Bit Size (BS): Measures the drill bit diameter; Depth (Depth): Represents the formation depth in meters; Data Transmission Log (DT): Provides data transmission information; Bulk Density Correction (DRHO): Corrects bulk density measurements; Effective Porosity (PHIF): Measures the effective porosity; Core Permeability (KLOG): Measures the core permeability; Net Reservoir Flag (NETS): Indicates net reservoir zones. These parameters are crucial for understanding the geological and petrophysical characteristics of the reservoirs in the Doba Basin, aiding in the optimisation of exploration and production strategies.

3.2. Methodology

To analyse lithological data and identify clays in well logs, we use the following steps.

First, identify the lithological character by analysing the Gamma Ray (GR) curve. According to Selley (1982) [15], clay-rich formations exhibit higher GR values, while non-clay formations show lower GR values. Typical thresholds include GR values ≥ 90 API for clays, ≤50 API for clean sands, and between 50 and 90 API for sandy-clay or clayey-sand zones.

Next, identify clays by examining various log responses. Al-Jafar *et al.* (2021) [16] suggest considering density-neutron scale compatibility and caliper logs for borehole enlargements. GR values should be high (≥90 API). Resistivity logs should show low resistivities (<20) with nearly overlapping curves. Neutron values (NPHI or TNPH) should be high (>20 or 30%). The N-D separation should be greater than in dolomites, and RHOB-NPHI separation should vary with compaction.

To estimate the clay volume, we apply the linear method to natural Gamma Ray logs, as suggested by Aquish and Gibson (1982) [17]. The clay volume (V_{sh}) is calculated using the formula:

$$V_{sh} = I_{GR} = \frac{GR_{read} - GR_{\min}}{GR_{\max} - GR_{\min}} \quad (1)$$

where,

GR_{read}: GR value of the bank read directly from the log (API);

$GR_{\min}$: Minimum GR value of the same bank (API); $GR_{\max}$: Maximum GR value of the same bank (API); I_{GR}: Gamma ray radiation index;

V_{sh}: Volume of shale.

The lithology computation method calculates up to four lithologies based on porosity efficiency, shale volume, water saturation, and bulk density. The apparent matrix properties (RHOma, DTma, and Uma) are calculated initially. For two lithologies, we use RHOma alone; for three lithologies, we incorporate DT and PEF/U; and for four lithologies, we use additional inputs and modify default lithologies, such as Quartz, Calcite, Dolomite, and Anhydrite, based on their specific properties [18].

We identify compact rocks (limestone, sandstone, and unfractured dolomite) by checking the caliper log for close-to-drill bit diameter readings, low GR values (<30), high resistivity values (>200), and density, neutron, and sonic values close to matrix values.

Specific lithologies like salt and anhydrite are identified by their caliper log, low GR values (<30), high resistivity values (>500), and specific density and neutron values.

We identify coal beds by looking for low GR values, high neutron values (>30%), low density (<2.0 g/cm^3), high sonic values (>90 μs/ft), and low resistivity values.

The obtained lithology is verified using the cross-plot technique, integrating neutron, density, and gamma ray log data [19]. Lithology is approximated using the Schlumberger Por-13 chart. The Density-Neutron-Gamma Ray cross-plot provides indications on the lithology and porosity of formations [16]. The super-

position of density and neutron curves also helps detect the nature of the formations traversed. The facies ratios are integrated into the cross-plot Density-Neutron-Gamma Ray parameter window using the Schlumberger chart, "Neutron porosity vs Bulk Density, NPHI", to obtain a more detailed view of the well layers (Table 1).

Table 1. Ratio of geological fascies used.

Fascies	Ratio
Limestone	20 < GR < 60 and 2.6 < RHOB < 2.7
Sandstone	15 < GR < 55 and 2.2 < RHOB < 2.6
Anhydride	−0.1 < NPHI < 0.1 and 2.7 < RHOB < 3.2
Salt	−0.1 < NPHI < 0.1 and 0 < RHOB < 2.4
Shale	0.15 < NPHI < 0.6 and 55 < GR < 300
Sand	RHOB > 2.6 and/or DeepRes > 500

We use the "Quick Look" interpretation method for rapid log analysis, focusing on delineating reservoir zones, determining WOC/WGC, identifying hydrocarbon types, lithology, porosity, water saturation, and water-oil contacts. This method is based on empirical relationships integrated into Techlog software [16] [20].

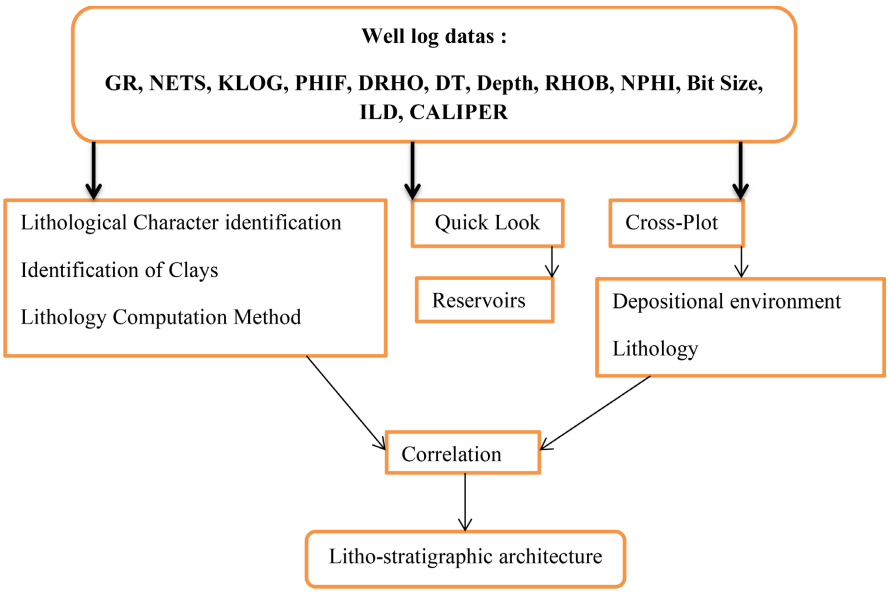

Figure 7. Flowchart of methodology used. Source: [4].

Finally, we correlate GR logs with stratigraphic depths and depositional environments as detailed in geological reports. Model representative stratigraphic formations that frequently appear in studied wells. We use gamma ray log cross-plots to represent the internal geological architecture of the area, integrating character-

istics of different formations.

The flowchart of the methodology used is given in Figure 7.

4. Results and Interpretation

4.1. Lithostratigraphy and Reservoir Delimitation

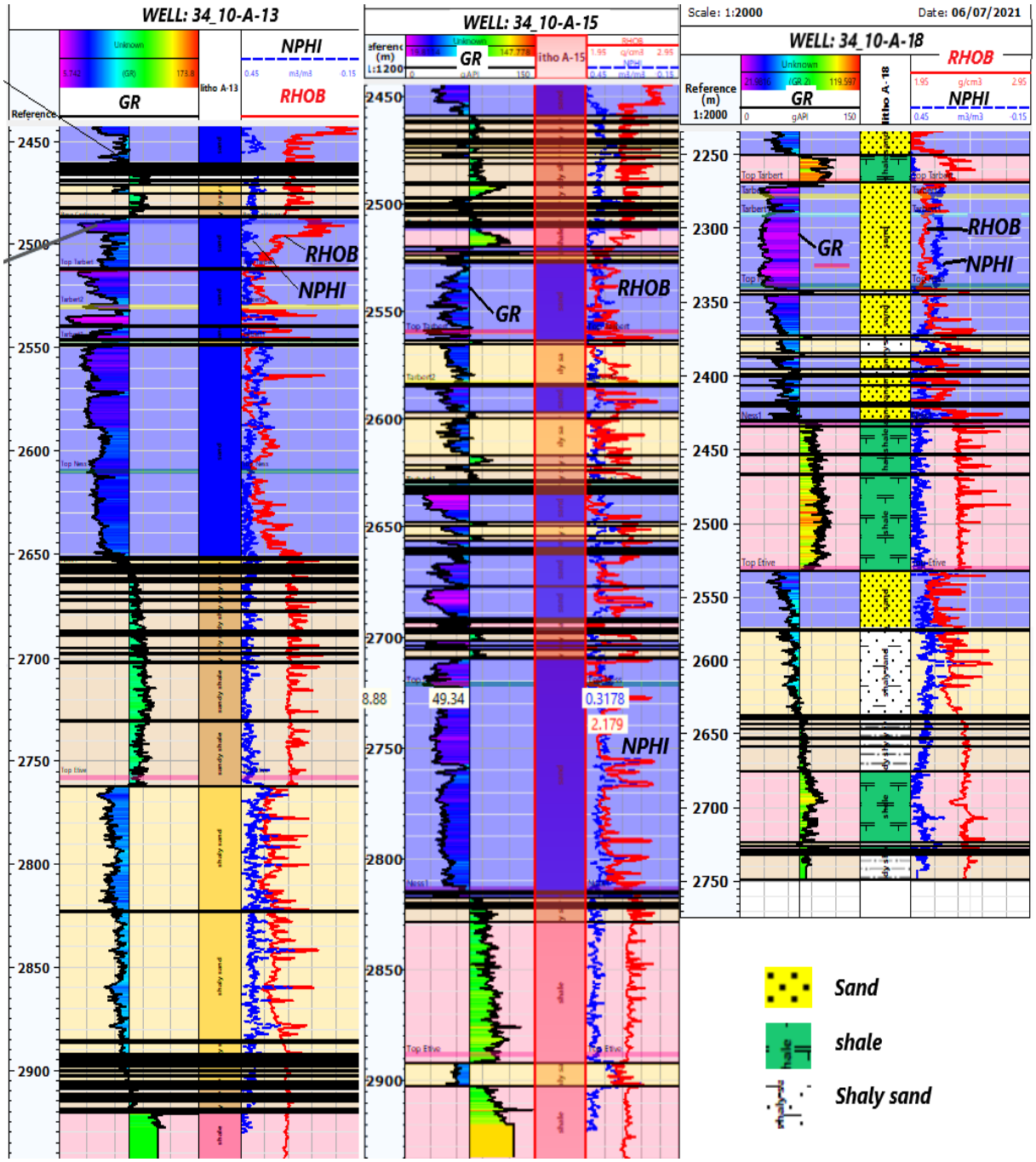

Figure 8. Lithological well log of well 34_10-A-13, 34_10-A-15, 34_10-A-18, showing shale and sand band. Source: [4].

Given the thicknesses of the sand and clay beds, we observe a significant percent-

age of clay and sand beds. Well 34_10-A-13 has a shale bed with a thickness of approximately 109 m and a sand bed of 160 m for the first section and 110 m for the second. Well 34_10-A-15 has a first shale bed with a thickness of approximately 100 m and the second of 80 m, with sand thicknesses of 40 m and 50 m. Well 34_10-A-18 has two shale beds with thicknesses of approximately 95 m and 100 m, and sand beds of approximately 100 m and 80 m. A more detailed study will provide specific characteristics of these observed clay and sand beds by delineating the reservoir levels of each well (Figure 8).

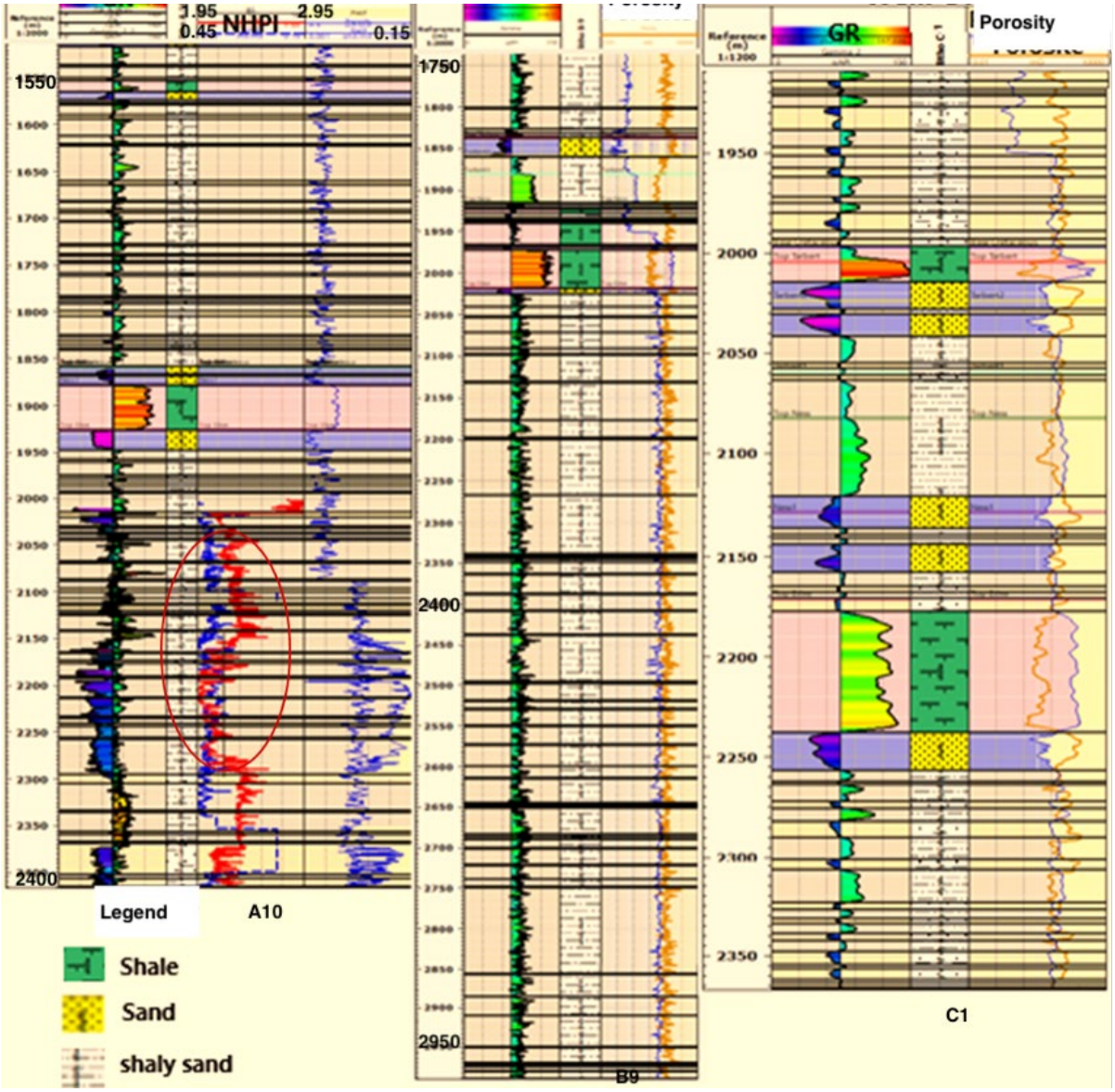

Figure 9. Lithological well log of well A10, B9 and C2 showing shale and sand ban. Source: [4].

Well A10 consists of two clay beds with thicknesses of 40 m and 64 m, and a sand bed with a thickness of approximately 154 m. In this well, the RHOB and NPHI logs intersect in the sand beds and diverge in the clay beds (area highlighted

in red) at a depth of approximately 2025 m. Well B9 consists of a single thin sand bed with a thickness of approximately 14 m and two clay beds with thicknesses of approximately 55 m and 39 m, followed by a significant sandy clay bed. Well C1 has three clay beds with thicknesses of approximately 20 m, 80 m, and 65 m, and sand beds with thicknesses of 25 m, 38 m, and 18 m. Porosity and permeability converge in the sandy-clay zones and diverge significantly in the zones with high clay and sand peaks (wells B9, C1) (**Figure 9**). Thickness details of shale and sand are given in **Table 2**.

Table 2. Ratio of geological fascies used.

Well	Shale thickness	Sand thickness
34_10-A-13	109 m	160 m
		110 m
34_10-A-15	100 m	40 m
	80 m	50 m
34_10-A-18	95 m	100 m
	100 m	80 m
A10	46 m	145 m
	64 m	
B9	55 m	14 m
	39 m	
C1	20 m	25 m
	80 m	38 m
	65 m	18 m

Well 34_10-A-13 consists of two potential reservoirs located at respective depths of 2510 - 2640 m for R1 and 2790-2885 m for R2, with thicknesses of 130 m and 95 m. They are separated by clay beds, with the nature of their cap rocks being largely composed of clay. Well 34_10-A-15 contains four reservoirs, with two potentially interesting ones located at depths of 2520 - 2555 m for R1, 2635 - 2653 m for R2, 2710 - 2815 m for R3, and 2890 - 2905 m, with thicknesses of 35 m, 18 m, 105 m, and 15 m. Reservoirs R1, R2, and R3 are separated by sandy clay and sandstone (**Figure 10**).

The well 30_10-A-18 comprises two reservoirs separated by clay and anhydrite beds, at depths of 2265 - 2422 meters for R1 and 2532 - 2633 meters for R2, with thicknesses of 157 meters and 101 meters, respectively. Well A10 is characterized by three reservoirs located at depths of 2019-2076 meters for R1, 2162 - 2280 meters for R2, and 2395 - 2416 meters for R3, with thicknesses of 57 meters, 118 meters, and 21 meters. Across all four wells, the RHOB and NPHI tend to intermix in the reservoir zones, reflecting the distribution of gas, oil, and water zones (**Figure 11**).

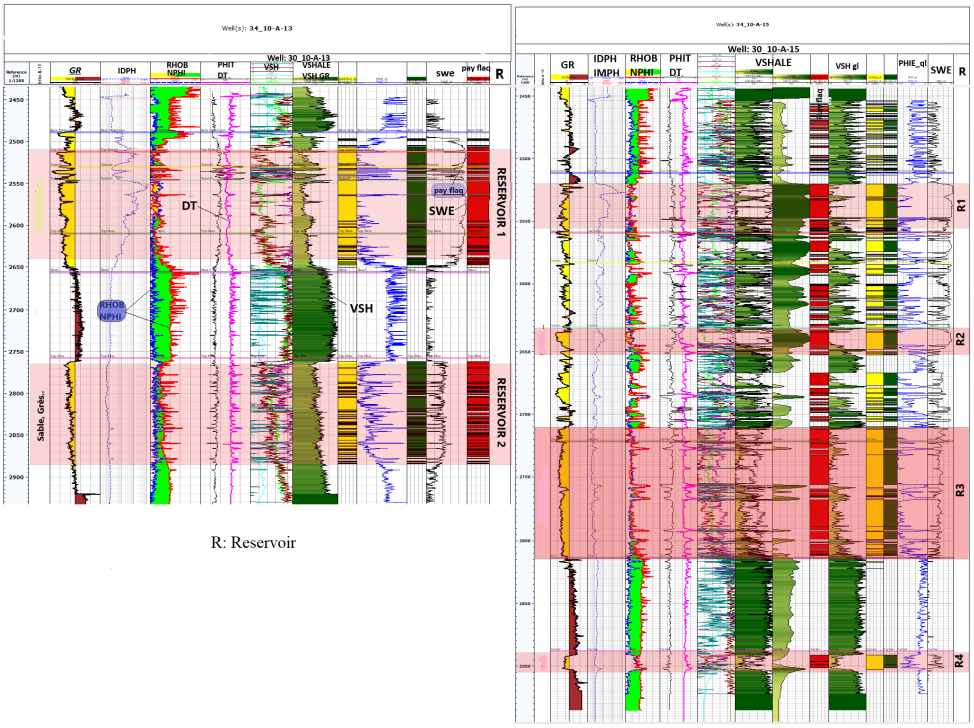

R: Reservoir

Figure 10. Reservoir identification of well 34_10-A-13 and 34_10-A-15 using Quick look. Source: [4].

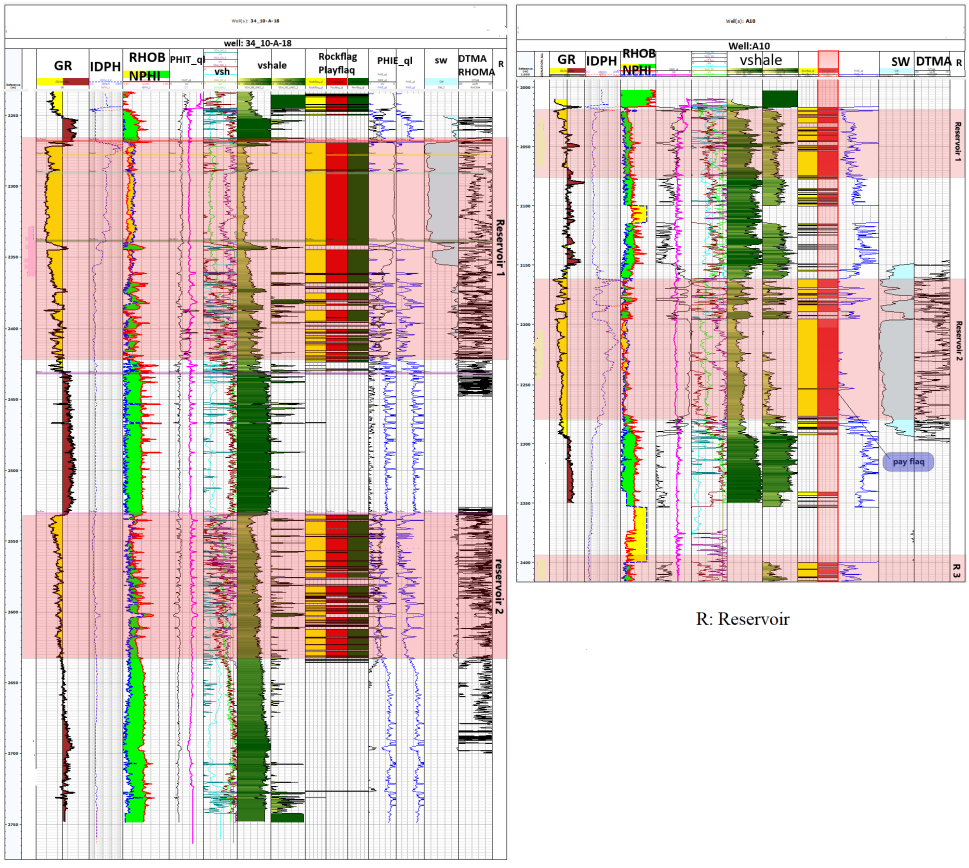

R: Reservoir

Figure 11. Reservoir identification of well 34_10-A-18 and A10 using Quick look. Source: [4].

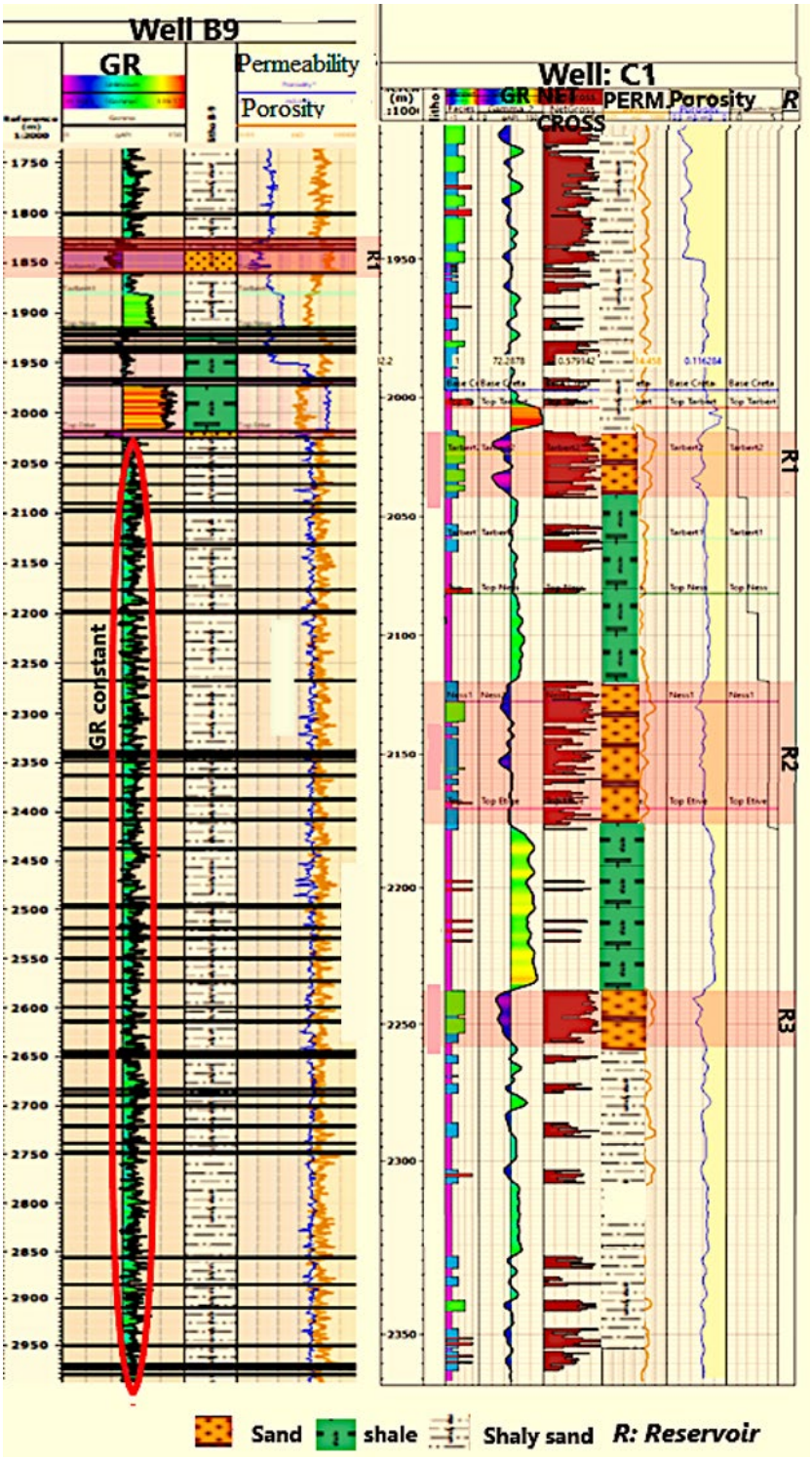

Figure 12. Reservoir identification of well B9 and C1 using Quick look. Source: [4].

Well B9 has low characteristics with thin sandy clay beds. It is characterised by a reservoir located between 1825 - 1855 m with a thickness of 30 m, followed by a long sandy clay bed extending from 2025 m to over 2950 m. Well C1 is characterized by three reservoirs located at depths of 2015 - 2042 m for R1, 2120 - 2176 m

for R2, and 2239 - 2258 m for R3, with thicknesses of approximately 27 m, 56 m, and 19 m. These reservoirs are separated by clay formations.

Well B9 consists of a single thin sand bed with a thickness of approximately 14 m and two clay beds with thicknesses of approximately 55 m and 39 m, followed by a significant sandy clay bed. Well C1 has three clay beds with thicknesses of approximately 20 m, 80 m, and 65 m, and sand beds with thicknesses of 25 m, 38 m, and 18 m. Porosity and permeability converge in the sandy-clay zones and diverge significantly in the zones with high clay or sand peaks (wells B9, C1) (**Figure 12**).

4.2. Cross-Plots and Depositional Environment

The neutron-density-gamma ray cross-plots for wells 34_10-A-13, 34_10-A-15, 34_10-A-18, and A10 allow for verifying and refining the lithology, and provide precision on the reservoir zones obtained from the Quick Look interpretation and the superposition of the neutron and density curves.

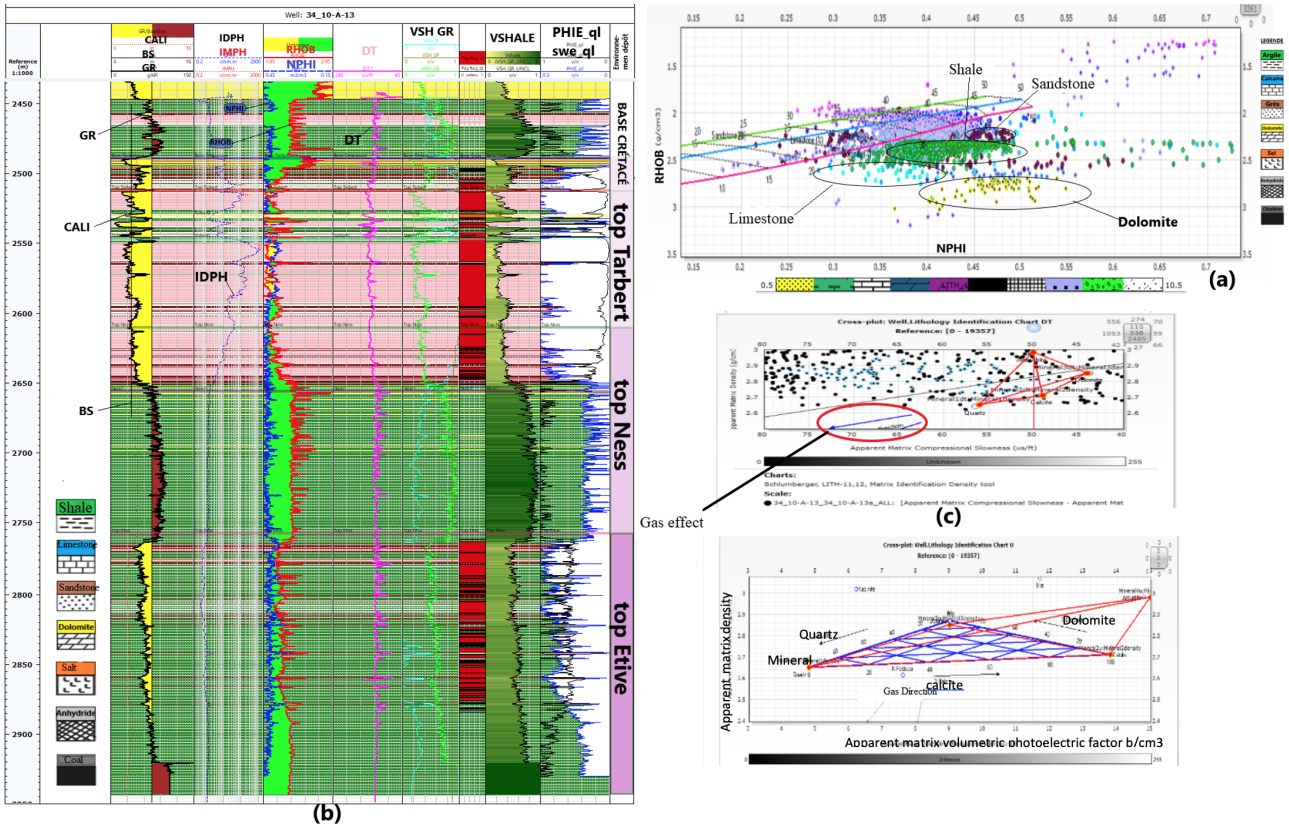

Figure 13. Cross-plots neutron-density-gamma ray of well 34 _10-A-13. Source: [4].

The interpretation of well 34_10-A-13 shows that, before the base of the Upper Cretaceous, this well is marked by alternating layers of dolomite, a low presence of sandstone, and a high percentage of clays (b). At the entry of the top Tarbert to Ness1, located at depth intervals of approximately 2500 - 2650 m, marked by ma-

rine processes, we observe a reservoir zone containing hydrocarbons (in pink) separated by a thin bed of clays and dolomite. The percentage of clays in these zones is low. The interval of approximately 2650 - 2780 m, from Ness1 to the top Etive in a non-marine environment, is marked by a high presence of clay, RHOB 2.60 g/cm^3, and a slight presence of dolomite. The top Etive interval in the upper shoreface or beach facies, ranging from approximately 2154 - 2945 m, shows a high percentage of clay (Figure 13).

The cross plot of well 34_10-A-15 show that, the interval from the base of the Cretaceous to the Ness1 at a depth of approximately 2555 - 2820 meters in a non-marine environment is characterised by a succession of reservoirs potentially containing hydrocarbons, marked by the presence of limestone, sandstone, clay, and coal, with a thickness of about 5 meters within the 2700 - 2705 meter interval, and the effect of gas (c) (Figure 14).

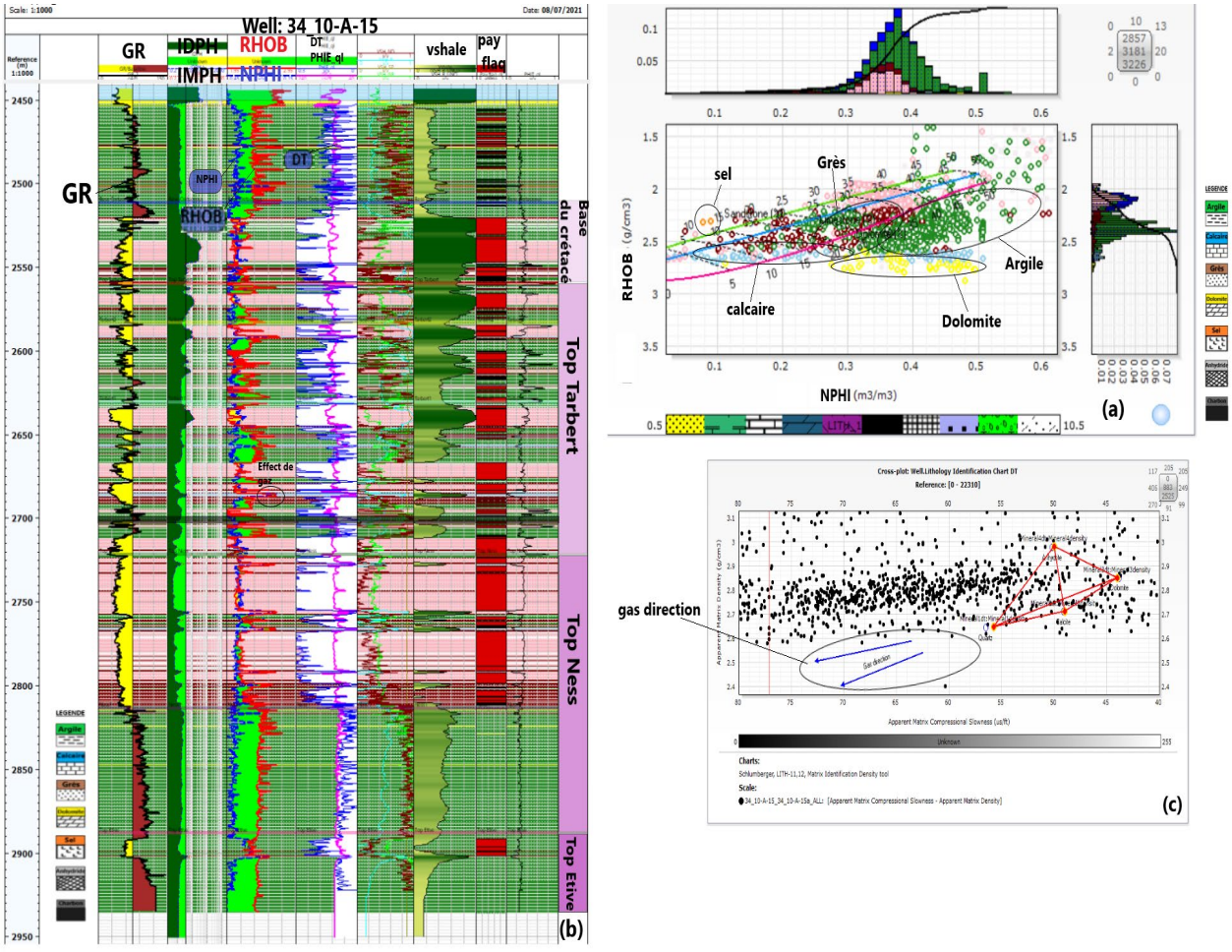

Figure 14. Cross-plots neutron-densité-gamma ray of well 34 _10-A-15. Source: [4].

The cross plot of well 34_10-A-18 shows that, from the base of the Cretaceous to the top Tarbert, we have an almost balanced alternation of sand and clay from the top Tarbert (b). At a depth of approximately 2370 m, we have a reservoir zone

characterised by a low presence of clay with a clear pay flag, in an environment influenced by marine processes, indicating a good reservoir containing hydrocarbons. The interval from Ness 1 to the top Etive is marked by a significant clay bed interspersed with some dolomites and sandstones with a gas effect (**Figure 15**).

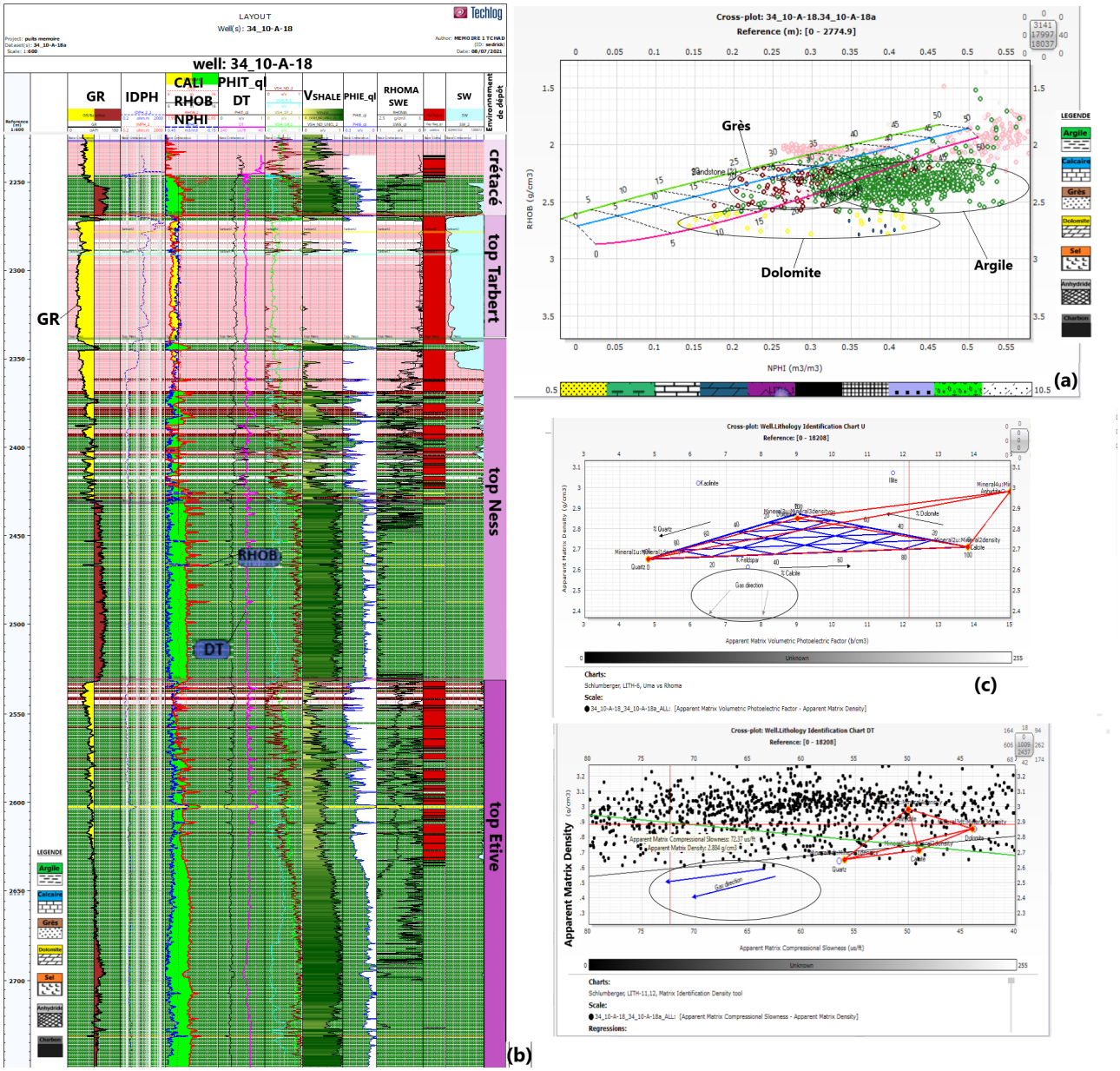

Figure 15. Cross-plots neutron-densité-gamma ray of well 34 _10-A-18. Source: [4].

The cross plot of well A10 shows that, unlike the other wells, A10 is recorded in the Etive interval, with a considerable and significant salt bed at (2100 - 2117 m) and (2357 - 2400 m) that serves as a cap rock for the reservoirs (b). The reservoir zones are located between 2160 - 2295 m with a low percentage of clay and a gas effect indicated by SW, with apparent matrix values of 70 us/ft for compression

and 1.5 g/cm^3 for density. We observe a high percentage of clays in these different wells using the GR-RHOB-NPHI analysis for values of (0.15 < NPHI < 0.6 and 55 < GR < 300). These clays consist of Kaolinite, chlorite, and montmorillonite (Figure 16).

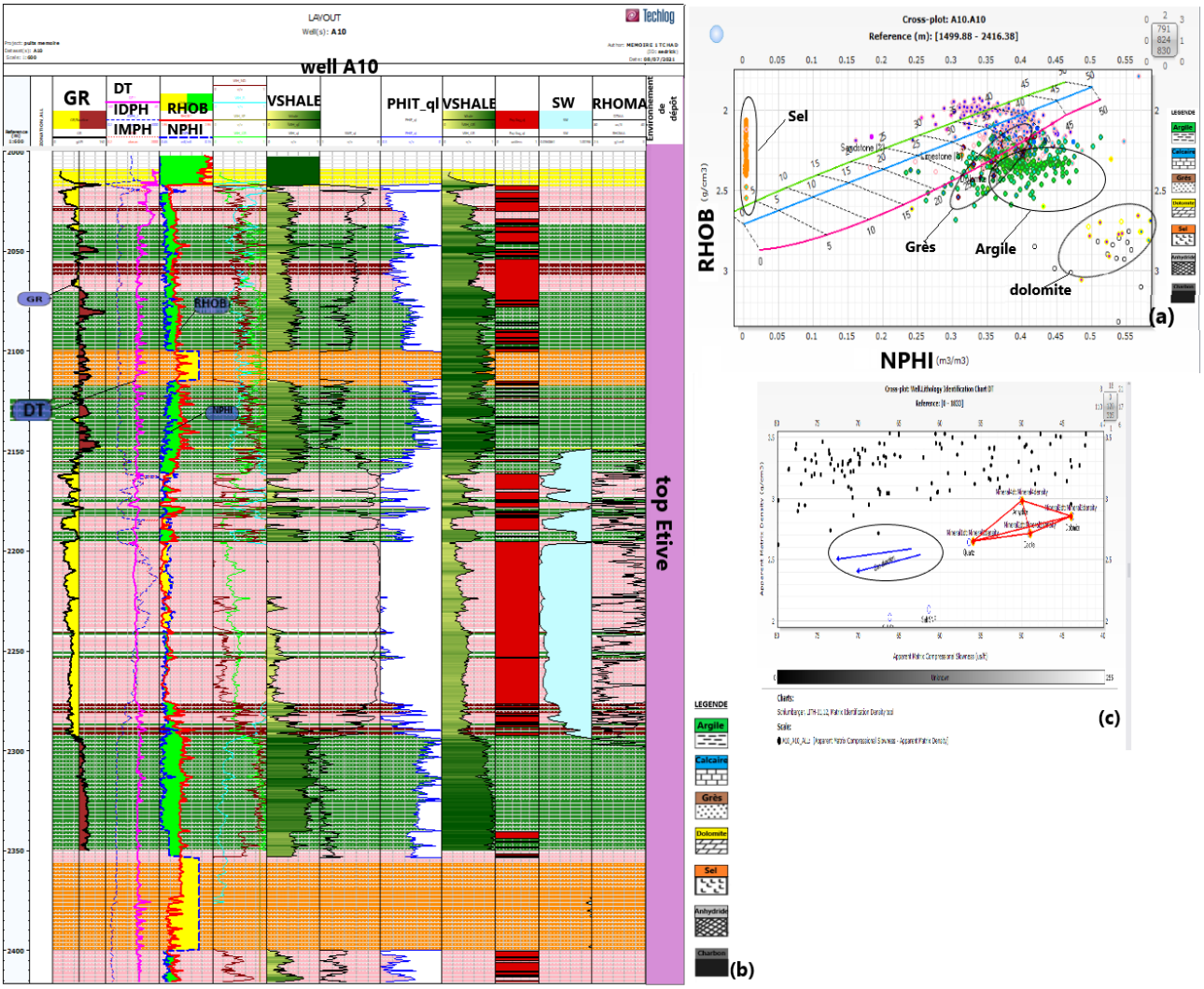

Figure 16. Cross-plots neutron-densité-gamma ray of well A10. Source: [4].

The cross plot of well B9 and C1 shows that the porosity-permeability-gamma ray cross-plots for wells B9 and C1 allow us to analyse the geological facies of these wells. In well B9 of Figure 15, we observe a Cretaceous base on the same line as the top Tarbert, which may be due to erosion or subduction. It has a potential reservoir at depths of 1850 m, with a thickness of approximately 30 m. In well C1, we identified three potential reservoirs, each separated by a thin clay bed with variations in permeability and porosity at that location. Porosity and permeability tend to vary in the clean clay and sand zones and remain constant in the sandy clay zones (Figure 17).

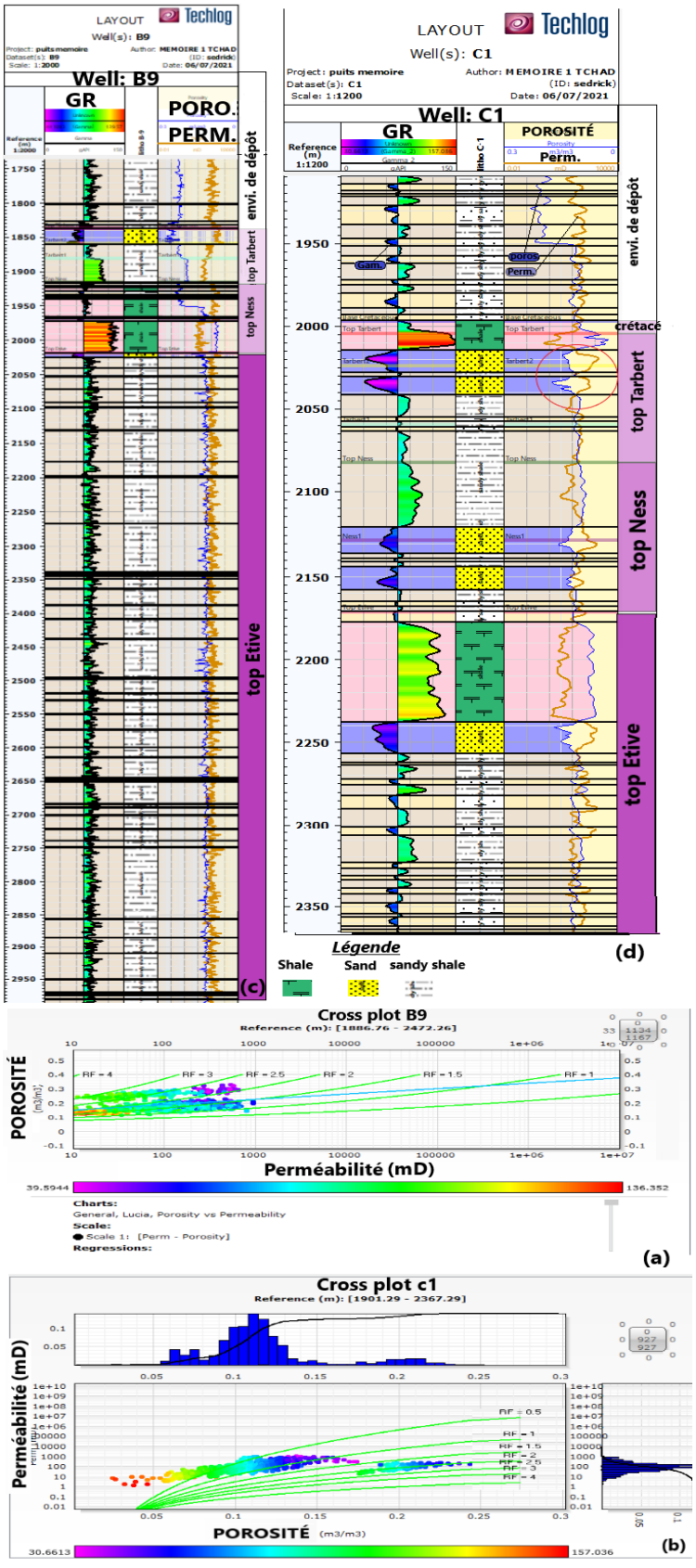

Figure 17. Cross-plots neutron-densité-gamma ray of well B9 and C1. Source: [4].

The Doba Basin, located in Chad, exhibits a complex depositional history primarily driven by its Late Mesozoic formation. The depositional environment is predominantly lacustrine (lake) and alluvial (river and stream-fed). The most updip alluvial facies are composed of coarse-grained to pebble-rich sandstones, formed as bar deposits within a broad braided fluvial system consisting of multiple low-sinuosity channels. These channels coalesce to form thick and laterally extensive channel complexes, with sandy flood-plain deposits containing lesser amounts of mud. The lacustrine facies belt is marked by terminal splay deposits accumulated along the lake margin and laminated silty mudstones within the lake center, laid down by suspension sedimentation. The thin terminal splay strata suggest a shallow ancestral lake basin with a relatively low gradient margin. The depositional and stratal architecture of the Upper Cretaceous strata is attributed to high-frequency climatic fluctuations (200- to 500-k.y. duration) imposed on longer-term climatic cycles (1 to 3 m.y.) and variable accommodation during late-stage extensional processes. These climatic conditions influenced the predictable temporal and spatial architectures of the alluvial systems. The basins experienced extension on a Pan African shear zone beginning in the Neocomian, with faults trending northeast-southwest and developing southeast-dipping half-grabens. Accommodation and relay zones created significant sediment input points. Inversion of Neocomian-age normal faults and the formation of northeast to southwest-trending anticlines are common, with maximum inversion of approximately 500 - 700 meters. The Late Oligocene to Early Miocene saw regional northeast-southwest extension, reactivating pre-existing Aptian-aged faults and forming new fault strands. Regional uplift associated with the African superplume created a widespread erosional surface around 10 Ma, erasing surface expressions of recent structures.

4.3. Correlation

Figure 18 shows that in the East, the wells encounter various types of lithology, with sand being more dominant in wells 34_10-A-13, 34_10-A-15, and 34_10-A-18, and less so in wells A10, B9, and C1 to the West. There is a notable presence of clay and sandy-clay in all the wells.

Before the base of the Cretaceous, in wells 34_10-A-13 and 34_10-A-15, there is a sand layer represented by the lime green color, which stops its continuity in other wells, possibly due to erosion or a fault.

At the base of the Cretaceous, the formation of sandy-clay layers composed of limestone, anhydrite, and evaporite is found in the top Tarbert of wells B9, A10, and C1, potentially characterizing the cap rocks. All wells are marked by a thick sand bed (34_10-A-13, 34_10-A-15, 34_10-A-18) that thins out in wells B9, C1, and A10. These thick sand beds may characterise potential reservoir rocks. In the Ness, the harmonious arrangement of clay beds consisting of medium to coarse sandstone across all wells was formed in a non-marine environment. In the Top Etive, the thick formation of sand beds in wells 34_10-A-18, 34_10-A-13, and B9,

and less developed in 34_10-A-15, 34_10-A-10, and C1, represents probable reservoir zones. Wells B9, C1, and 34_10-A-10 subsequently present a significant sandy-clay bed that is absent in the other wells, possibly due to a lack of recorded log data.

The analysis of this figure reveals that sand/sandstone and sandy-clay are the dominant formations in all the studied wells. Additionally, the sand-dominant wells 34_10-A-13, 34_10-A-15, and 34_10-A-18 show several clean clay beds with occasional fine sandstone traces. However, in wells B9, C1, and 34_10-A-10, sand beds are less represented, with an abundant presence of sandy-clay elements. Reservoirs with thick layers can be considered good reservoirs containing hydrocarbons.

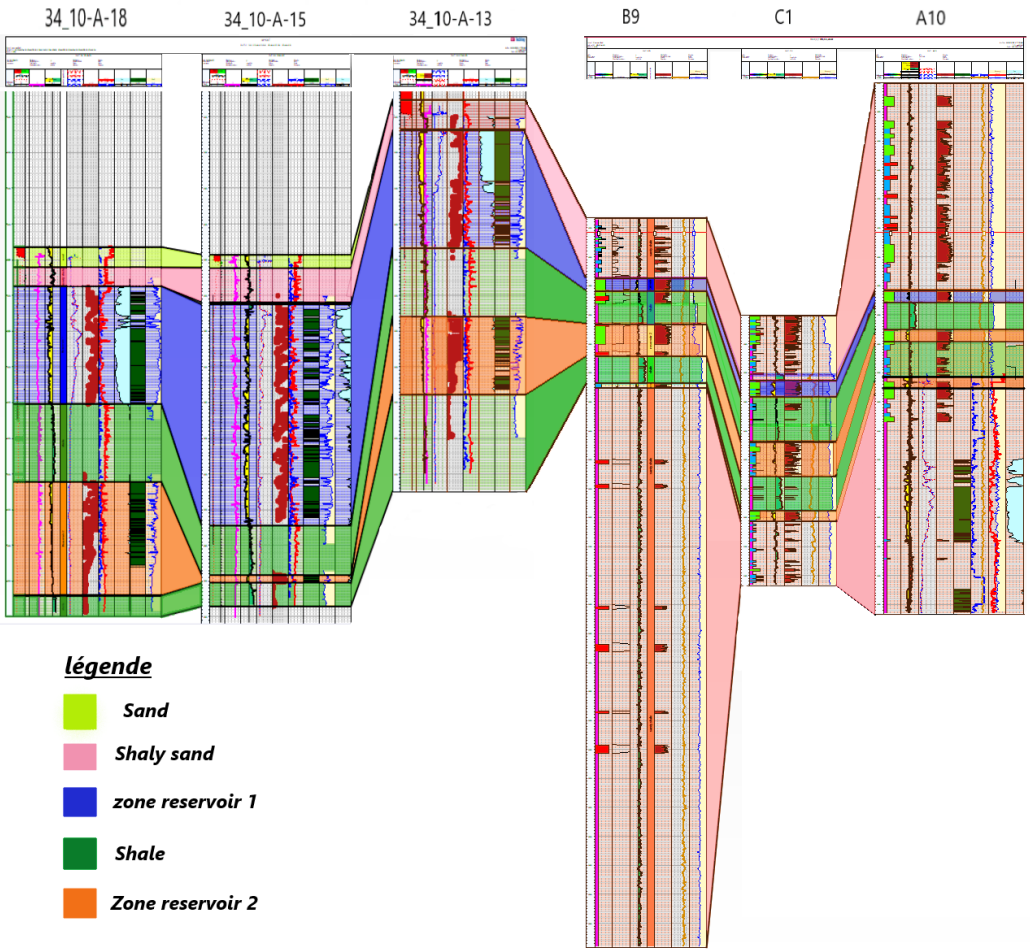

Figure 18. Lithological correlation of well. Source: [4].

4.4. Discussion

The structural evolution of the Doba Basin is deeply influenced by tectonic activity, particularly the inversion of Neocomian-age normal faults, which led to the formation of northeast-southwest trending anticlines and compartmentalized reservoirs [2] [21]. These tectonic features not only shaped the basin's geometry but

also enhanced reservoir quality by increasing porosity and permeability through fracturing and thermal uplift. Concurrently, the spatio-temporal variation in lithofacies reflects a transition from marine to non-marine deltaic and lacustrine environments, driven by climatic fluctuations and tectonic pulses [22] [23]. The interbedded sand, shale, and clay layers, along with radioactive sands that complicate log interpretation, indicate dynamic depositional settings with high-frequency sedimentation cycles. Reservoir intervals are notably present at average depths of 250 m, characterized by coarse to fine-grained sandstones with clay cement, some reaching thicknesses over 30 m, while deeper zones, like in well B9, show weaker reservoir characteristics due to sandy clays and structural disruptions such as the top Tarbert event. Despite these complexities, the basin's lacustrine deposits and fault-related traps underscore its high hydrocarbon potential [24].

5. Conclusion

Our analysis employed various methods, including cross-analysis and cross plots from resistivity (RHOB) and neutron density (NPHI) logs, to gather critical insights into the depositional environments. The geometric structure of the wells was meticulously designed by identifying reservoir constituents and cap rocks. Detailed lithological descriptions of the upper and lower parts of the Cretaceous formation reveal thick clay deposits, especially in the Ness—top Etives intervals, formed in a non-marine delta plain environment. These deposits are interbedded with porous sandstone, fine to coarse sand, dolomite, coal, and salt. Potential reservoirs were identified in marine environments with gas effects generated from type II organic matter and non-marine lacustrine environments like Ness, which generate type I and III organic matter. This study fills a crucial gap in the literature by providing detailed geological and petrophysical parameters for the Doba Basin formation, which were previously less understood. It enhances our understanding of the lithology and hydrocarbon potential in the Cretaceous formations of this area, offering valuable insights for future exploration and development efforts. The findings underscore the significant hydrocarbon prospects in the studied reservoirs, highlighting their excellent porosity and permeability characteristics.

Acknowledgements

The authors would like to express their deepest and sincere thanks to Diab Ahmad Diab for the facilities provided during the data acquisition for this work.

Conflicts of Interest

The authors declare no conflicts of interest regarding the publication of this paper.

References

[1] Wang, L., Hu, Y., Zhang, G., Wang, L., Zhang, X. and Liang, Q. (2022) Hydrocarbon Accumulation Pattern and Exploration Direction in Southern Chad Basin. In: Lin, J.,

Ed., *Springer Series in Geomechanics and Geoengineering*, Springer, 995-1004. https://doi.org/10.1007/978-981-19-2149-0_89

[2] Dou, L., Xiao, K., Du, Y., Wang, L., Zhang, X., Cheng, D., *et al.* (2022) Exploration Discovery and Hydrocarbon Accumulation Characteristics of the Doseo Strike-Slip and Inverted Basin, Chad. *Petroleum Exploration and Development*, **49**, 247-256. https://doi.org/10.1016/s1876-3804(22)60021-1

[3] Bouteyre, G., Cabot, J. and Dresch, J. (1964) Observations sur les formations du continental terminal et du Quaternaire dans le bassin du Logone (Tchad). *Bulletin de la Société Géologique de France*, **7**, 23-27. https://doi.org/10.2113/gssgfbull.s7-vi.1.23

[4] Ahmad, D.A., Domra, K.J., Abdelhakim, B. and Oyoa, V. (2022) The Use of Integrated Geophysical Methods to Assess the Petroleum Reservoir in Doba Basin, Chad. *Advances in Science, Technology and Engineering Systems Journal*, **7**, 34-41. https://doi.org/10.25046/aj070406

[5] Nur Fathiha, M.S., Lo, S.Z. and Ahmed Mohamed, A.S. (2017) Reservoir Characterization of Lacustrine Environment, Doba Basin, Southern Chad: Radioactive Sand Delineation. In: Awang, M., Negash, B., Md Akhir, N., Lubis, L., Md. and Rafek, A., Eds., *ICIPEG* 2016, Springer, 337-349. https://doi.org/10.1007/978-981-10-3650-7_29

[6] Patterson, P.E., Jones, C.R. and Skelly, R.L. (2010) Sequence Stratigraphy of Alluvial Systems: Chapter 7. In: Abreu, V.D., Neal, J., Bohacs, K. and Kalbas, J., Eds., *Sequence Stratigraphy of Siliciclastic Systems: The Exxon Mobil Methodology: Atlas of Exercises*, SEPM Concepts in Sedimentology and Paleontology, 131-143.

[7] Genik, G.J. (1993) Petroleum Geology of Cretaceous-Tertiary Rift Basins in Niger, Chad, and Central African Republic. *The AAPG Bulletin*, **77**, 1405-1434.

[8] Pan, X., Yuan, S., Ji, Z., Hu, G. and Liu, L. (2013) Forming Mechanism and Petroleum Geological Features of the Western-Central African Rift Basins (WCARBs). *International Petroleum Technology Conference*, Beijing, 26-28 March 2013, IPTC-17116-MS.

[9] Dou, L., Wang, J., Wang, R., Wei, X. and Shrivastava, C. (2018) Precambrian Basement Reservoirs: Case Study from the Northern Bongor Basin, the Republic of Chad. *AAPG Bulletin*, **102**, 1803-1824. https://doi.org/10.1306/02061817090

[10] Warren, M.J. (2009) Tectonic Inversion and Petroleum System Implications in the Rifts of Central Africa. Jenner GeoConsulting, CSPG SCEG CWLS Convention.

[11] Fairhead, J.D., Green, C.M., Masterton, S.M. and Guiraud, R. (2013) The Role That Plate Tectonics, Inferred Stress Changes and Stratigraphic Unconformities Have on the Evolution of the West and Central African Rift System and the Atlantic Continental Margins. *Tectonophysics*, **594**, 118-127. https://doi.org/10.1016/j.tecto.2013.03.021

[12] Moss, B. (1992) The Etive Formation: Depositional Environments and Sedimentology. *Geological Society*, **61**, 123-135.

[13] Aremu, M. (2015) Chad Prepares to Be an Oil Producers. Oil and Gas Online. http://www.oilandgasonline.com/doc/chad-prepares-to-be-an-oil-producer-0001

[14] Genik, G.J. (1992) Regional Framework, Structural and Petroleum Aspects of Rift Basins in Niger, Chad and the Central African Republic. *Tectonophysics*, **213**, 169-185. https://doi.org/10.1016/b978-0-444-89912-5.50036-3

[15] Selley, R.C. (1982) An Introduction to Sedimentology. Academic Press.

[16] Al-Jafar, M.K. and Al-Jaberi, M.H. (2021) Determination of Clay Minerals Using Gamma Ray Spectroscopy for the Zubair Formation in Southern Iraq. *Journal of Petroleum Exploration and Production Technology*, **12**, 299-306. https://doi.org/10.1007/s13202-021-01371-3

[17] Asquith, G.B. and Gibson, C.R. (1982) Basic Well Analysis for Geologist. AAPG.

[18] Guo, Y., Li, Z., Lin, W., Zhou, J., Feng, S., Zhang, L., *et al.* (2023) Automatic Lithology Identification Method Based on Efficient Deep Convolutional Network. *Earth Science Informatics*, **16**, 1359-1372. https://doi.org/10.1007/s12145-023-00962-4

[19] Meunier, M. (2011) Diagraphie différée. IFP Training, 135-148.

[20] Serra, O. (1986) Sedimentary Environments from Wireline Logs Schlumberger. 2nd Edition, Shlumberger Limited, 238-243.

[21] Reynolds, D.J. and Jones, C.R. (2004) Tectonic Evolution of the Doba and Doseo Basins, Chad: Controls on Trap Formation and Depositional Setting of the Three Fields Area, Chad. https://www.searchanddiscovery.com/documents/abstracts/2004hedberg_baku/extended/reynolds/reynolds.htm

[22] Patterson, P.E., Jones, C.R. and Skelly, R.L. (2006) Climatic Controls on Depositional Setting and Alluvial Architecture, Doba Basin, Chad (ABS.). AAPG Abstracts with Program, 76-82.

[23] Patterson, P.E., Skelly, R.L. and Jones, C.R. (2012) Climatic Controls on Depositional Setting and Alluvial Architecture, Doba Basin, Chad. In: Baganz, O.W., Bartov, Y., Bohacs, K. and Nummedal, D., Eds., *Lacustrine Sandstone Reservoirs and Hydrocarbon Systems*, American Association of Petroleum Geologists, 265-298. https://doi.org/10.1306/13291393m953237

[24] Patterson, P.E., Jones, C.R., Schellpeper, M.E., Skelly, R. and Lowe, D. (2004) Climatic evolution of Doba Basin, Chad: Controls on Depositional Setting and Stratal Architecture of the Three-Fields Areas, Chad. 2004 *AAPG Hedberg Conference on Sandstone Deposition in Lacustrine Systems*, Baku, 12-16 June 2004, 2 p.